Regular article

Mechanisms and preliminary validation of luteolin in the treatment of hyperuricemia based on network pharmacology and toxicology studies

Yulin Hong†, Xinhui Yang†, Zhenyu Liu, Yizhen Chen, Yunkun Zhang, Xin Wu*

School of life science and biopharmaceutics, Shenyang Pharmaceutical University, Shenyang 110016, China

Abstract

Hyperuricemia (HUA) refers to a condition where fasting serum uric acid levels exceed 420 μmol/L in men and 350 μmol/L in women, affecting 17.4% of China's general population, showing increasing prevalence among younger individuals. Luteolin, a common flavonoid compound, exhibits multiple biological effects, including inhibition of tumor proliferation and inflammatory responses. It also suppresses the activity of urate transporter 1 (URAT1), promoting uric acid excretion. This study is the first to integrate network toxicology and network pharmacology approaches to systematically analyze the multi-target mechanisms of adenine-induced HUA and luteolin-treated HUA, with molecular docking validation of interaction targets. We constructed compound-pathway-intersection gene networks and a dual-group PPI network to analyze the mechanisms of adenine-induced HUA and luteolin-treated HUA. The dual-group PPI network identified 7 shared targets, namely XDH, PYGL, IL10, PPARG, TNF, VEGFA, and MAOA, involving core intersecting pathways such as purine-xanthine metabolism and insulin resistance. Luteolin may activate PPARG to regulate inflammation and uric acid excretion modules in the adenine network. GO-KEGG analysis indicates that intersection genes for adenine pathogenesis involve diverse biological processes, cellular components, and molecular functions, with core target KEGG analysis revealing 15 signaling pathways. Luteolin's therapeutic targets are associated with more entries, and its core target KEGG analysis identified 46 signaling pathways. Molecular docking shows TNF, PPARG, and PYGL bind to both luteolin and adenine with negative binding energies, and luteolin's binding energies are all below 5 kJ/mol, confirming stable binding. Luteolin's anti-HUA mechanism is characterized by inhibition of production, promotion of excretion, anti-inflammation and metabolic regulation, but interactions with gut microbiota metabolites require further study.

***Keywords*:** hyperuricemia (HUA); luteolin; network pharmacology; network toxicology; molecular docking

1 Introduction

Hyperuricemia is a metabolic disorder with multiple etiological factors. Previous studies have established correlations between hyperuricemia and renal dysfunction, cardiovascular diseases, and insulin resistance. Contributing factors include

† These authors contributed equally to this work and should be considered co-first authors.

* Author to whom correspondence should be addressed. Address: School of Life Science and Bioharmaceutics, Shenyang Pharmaceutical University, 103 Wenhua Road, Shenyang 110016, China; Tel.: +86-24-43520921; E-mail: wuxin44771@163.com.

These authors have no conflict of interest to declare.

Received: 2025-06-20 Accepted: 2025-08-01

dietary habits, genetic predisposition, age, and organ dysfunction, though the precise mechanisms require further elucidation [1]. The global prevalence of hyperuricemia has risen markedly in recent years, underscoring the need for more research [2]. Emerging evidence suggests luteolin possesses therapeutic potential against hyperuricemia. Therefore, we adopted network pharmacology and network toxicology approaches to systematically analyze and preliminarily validate its mechanisms and potential targets of luteolin in hyperuricemia treatment.

Uric acid, the end product of purine metabolism, originates primarily from endogenous purine nucleotide metabolism and dietary intake. Its excretion is mainly handled by the kidneys and intestines [3]. Abnormally elevated serum uric acid levels occur when excretion falls below production. Hyperuricemia (HUA) is clinically defined when fasting serum uric acid levels exceed 420 μmol/L in men or 350 μmol/L in women [4]. In China, the prevalence among the general population is 17.4%, with notable regional, gender, and age disparities. Strikingly, the highest prevalence is observed in the 18–29 age group, indicating a trend toward younger demographics [5,6]. Consequently, identifying effective therapeutic approaches for hyperuricemia has become a critical research focus.

Luteolin (3′,4′,5,7-tetrahydroxyflavone), a naturally occurring flavonoid, is widely distributed in plants including broccoli, green peppers, dandelions, and mint [7]. It demonstrates multiple biological effects, such as inhibiting tumor proliferation, suppressing inflammatory responses, and attenuating oxidative stress. Importantly, studies confirm that luteolin inhibits the activity of urate transporter 1 (URAT1), promoting uric acid excretion and thereby alleviating hyperuricemia [8].

Advances in systems biology have popularized network pharmacology and network toxicology. Network pharmacology, an emerging interdisciplinary field rooted in systems biology, focuses on the systematic analysis of drug molecules. Conversely, network toxicology investigates toxicity-target-drug interactions, utilizing network-based approaches to predict adverse drug effects [9]. Both disciplines leverage networked relationships among proteins, pathways, and diseases to analyze drug likeness, facilitating the discovery of potential drug targets and elucidating drug-target interactions [10].

2 Materials and methods

2.1 Network toxicology prediction

2.1.1 Compound retrieval and toxicity analysis

Querry the PubChem (https://pubchem.ncbi.nlm.nih.gov/) database, using “adenine” as the search term. Prioritize selection of experimentally validated structures, excluding duplicates and entries with low-confidence scores. Download the standardized SMILES structural formula of the confirmed structure and import it into the ADMETlab 3.0 (https://admetlab3.scbdd.com/server/screening) and Protox (https://tox.charite.de/protox3/) platforms for toxicity analysis.

2.1.2 Compound target prediction

Import the SMILES structure into the ChEMBL (https://www.ebi.ac.uk/chembl/), STITCH (https://ngdc.cncb.ac.cn/databasecommons/database/id/208), and SwissTargetPrediction (http://swisstargetprediction.ch/) databases. Combine the target prediction results from all databases, filter out targets with probability < 0.1, and remove duplicates to obtain the final compound target list.

2.1.3 Disease gene acquisition

Querry GeneCards (https://www.genecards.

org/), OMIM (https://www.omim.org/), and DrugBank (https://go.drugbank.com/) databases, using "Hyperuricemia" as the search term. After removing low probability (Score ≤ 0.4) and duplicates, construct the disease gene set.

2.1.4 Compound-disease intersection genes

Employ the Wei Sheng Xin platform (https://pharm.ncmi.cn/) to process disease-related and compound-related genes. Import both gene sets into the platform's Venn diagram module to generate a compound-disease intersection gene Venn diagram.

2.1.5 Intersection gene PPI network construction

Submit the intersection genes to the STRING database (https://string-db.org/; Species: Homo sapiens). Following PPI network prediction, adjust filtering parameters and export the results as a TSV file. Visualize and analyze the network in Cytoscape 3.9.1 (https://cytoscape.org/release_notes_3_9_1.html).

2.1.6 Core target screening

Open the TSV file and analyze network parameters, including Degree Centrality (DC), Betweenness Centrality (BC), and Closeness Centrality (CC), using the built-in CentiScaPe 2.2 tool (https://apps.cytoscape.org/apps/centiscape). Screen nodes with DC, BC, and CC values exceeding their respective thresholds. Generate a core subnetwork to identify key targets mediating adenine-induced hyperuricemia pathogenesis.

2.1.7 GO-KEGG enrichment analysis

Submit the intersection genes to the DAVID Functional Annotation Tool (https://david.ncifcrf.gov/). Extract and rank results by Count value (highest to lowest) for Gene Ontology (GO) terms, namely Biological Process (BP), Cellular Component (CC), and Molecular Function (MF), and KEGG Pathway entries (https://www.genome.jp/kegg/). Retain the top 10 entries in each category for subsequent analysis and visualization.

2.1.8 Compound-pathway-intersection gene network construction

Construct an "Adenine-Hyperuricemia Compound-Pathway-Intersection Gene" network using Cytoscape 3.9.1 (https://cytoscape.org/release_notes_3_9_1.html). Nodes represent compounds, targets, intersection genes, and diseases; edges denote their interrelationships. Calculate key node attributes using network analysis tools, with distinct shapes or colors differentiating relationships to identify critical components and target interactions.

2.2 Network pharmacology prediction

Retrieve the SMILES structure of luteolin from the PubChem (https://pubchem.ncbi.nlm.nih.gov/) database and input it into the SwissTargetPrediction (http://swisstargetprediction.ch/) database to identify its related genes. Use a Venn diagram to identify the intersection between luteolin's predicted targets and HUA-related targets; these overlapping targets serve as potential therapeutic targets for luteolin in treating HUA. Construct a protein-protein interaction (PPI) network of the potential therapeutic targets using the STRING (https://string-db.org/) database and Cytoscape 3.9.1 (https://cytoscape.org/release_notes_3_9_1.html) software to identify core therapeutic targets. Perform Gene Ontology (GO) and Kyoto Encyclopedia of Genes and Genomes (KEGG) enrichment analyses on the key signaling pathways of potential therapeutic targets using the DAVID (https://david.ncifcrf.gov/) database, and build a "luteolin-pathway-intersection gene" network diagram using Cytoscape 3.9.1 software.

2.3 Molecular docking

Within the PPI network, the representative core therapeutic target TNF was selected as the receptor, and HUA-modeling compound adenine and potential therapeutic compound luteolin were selected as ligands for molecular docking. First, locate the protein structures of TNF, PPARG, and PYGL in the UniProt (https://www.uniprot.org/) database, and download their corresponding 3D structure files (PDB format) from the Protein Data Bank (PDB, https://www.rcsb.org). Use PyMOL 2.5 (https://pymol.org/) to remove water molecules, heteroatoms, and non-essential chains from the structures, saving them as preprocessed protein files (e.g., TNF_clean.pdb). Retrieve the 2D structures of ligand molecules from the PubChem (https://pubchem.ncbi.nlm.nih.gov/) database in SDF format, convert them to PDB format using Open Babel 3.1.1 (https://openbabel.org/docs/Installation/install.html), and perform molecular docking with AutoDock 4 (https://autodock.scripps.edu/). Export docking results and import them for 3D visualization analysis. Binding energy < 0 kJ/mol indicates spontaneous ligand-receptor binding, while binding energy < -5 kJ/mol indicates stable docking.

3 Result

3.1 Analysis of the joint results of cyber-toxicology and cyber-pharmacology

3.1.1 Compound-related target screening

Using ChEMBL, STITCH, and SwissTarget-Prediction databases with a probability score > 0.1 threshold, 523 targets of the compound adenine were obtained. Applying identical criteria through SwissTargetPrediction database also yielded 152 luteolin targets.

3.1.2 Disease gene acquisition

Using “Hyperuricemia” as the search term, disease-associated targets were identified from GeneCards, OMIM, and DrugBank. After applying a relevance score ≥ 0.4 and removing duplicates, 323 targets were obtained. This target set encompasses not only core regulatory factors in uric acid metabolism pathways but also key genes involved in pathological processes such as inflammatory responses and oxidative stress, thereby providing a comprehensive molecular framework for elucidating the multidimensional pathogenesis of hyperuricemia. The establishment of this target collection lays a critical data foundation for subsequent investigations into multi-target mechanisms of compound action and cross-disease comorbidity gene association.

3.1.3 Compound-disease intersection gene analysis

Based on the previously established target profile of HUA, this study employed the Wei Sheng Xin bioinformatics analysis platform to investigate the interaction mechanisms between adenine, luteolin, and HUA. Multi-dimensional cross-gene mapping analysis identified 40 shared targets between adenine and HUA and 15 intersecting genes between luteolin and HUA. These cross-target sets provide direction for subsequent molecular docking studies (Fig. 1A-B).

3.1.4 Dual-group PPI network construction and pharmacological mechanism comparison

To systematically analyze the pathogenic mechanisms of adenine-induced HUA and the potential pharmacological effects of luteolin against HUA, this study imported the screened 40 adenine-induced HUA core genes and 15 luteolin anti-HUA therapeutic targets into the STRING database to

construct a dual-group protein-protein interaction (PPI) network. Key parameters were uniformly set: interaction confidence ≥ 0.7 (high confidence), interaction sources (experiments, databases, and text-mining), and exclusion of disconnected nodes. Results are shown in Table 1 and Fig. 1C-D.

Table 1 Dual-group PPI network construction results

Network type	Number of nodes	Number of edges	Average node degree	Local clustering coefficient	PPI enrichment *P*-value
Adenine	40	123	6.15	0.563	< 1.0e-16
Luteolin	15	43	5.73	0.772	3e-09

According to the dual-network interaction mechanism, a total of 7 shared targets were identified: XDH, PPARG, TNF, VEGFA, IL10, PYGL, and MAOA. These targets implicate core intersecting pathways, purine-xanthine metabolism (XDH-PYGL) and PPAR signaling pathway (PPARG-ABCG2 in the luteolin network and PPARG-ABCB11 in the adenine network). This suggests that luteolin may activate PPARG to concurrently regulate inflammation modules and uric acid excretion modules in the adenine network, inhibiting TNF/IL10 and upregulating ABCG2 to compensate for SLC22A1 dysfunction.

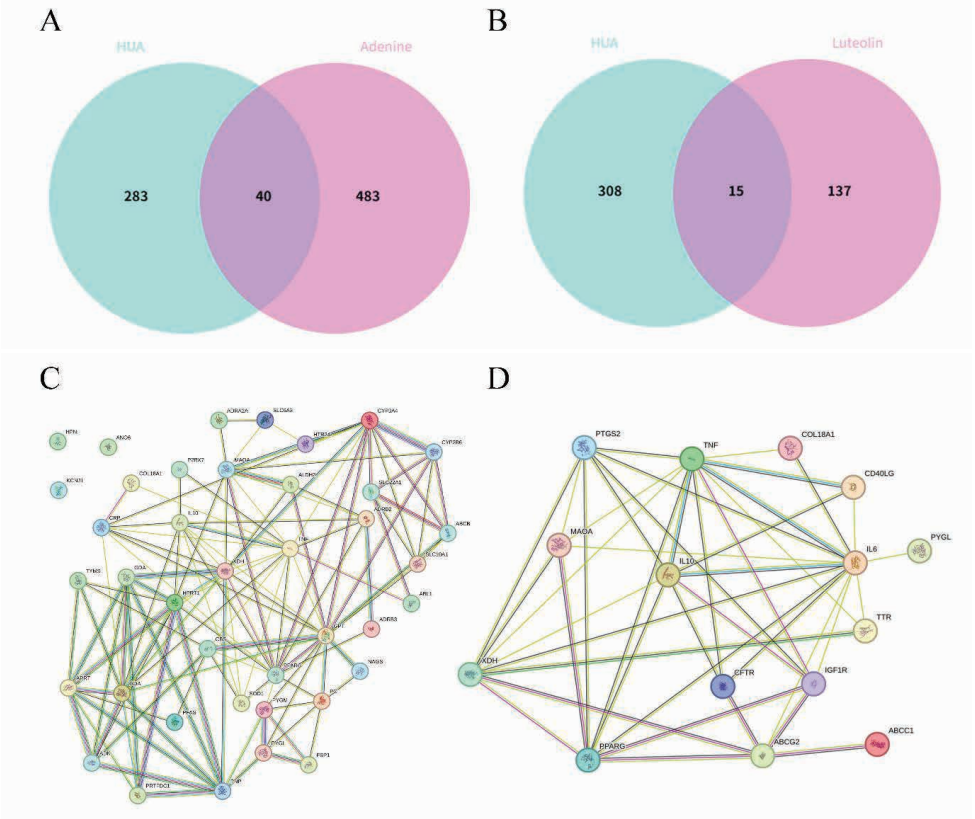

Fig. 1 Group diagram of the compounds-disease relationship. Left: adenine; Right: luteolin (A-B) Venn diagram of intersection gene between disease gene and Adenine-related targets or luteolin-related targets; (C-D) PPI network diagram of intersection gene (protein) between disease and compounds

3.1.5 Core target screening results

For adenine-induced hyperuricemia pathogenesis, the PPI network of 40 common targets was constructed in STRING. Using the CentiScaPe-2.2 plugin, 10 core proteins (e.g., GPT, TNF, XDH, PPARG, ADA) were identified based on network topology parameters (Table 2, Fig. 2A-B).

For luteolin's therapeutic targets against HUA, 3 core targets (IL-6, TNF, ABCG2) were identified from 15 common genes using Degree Centrality (DC), Betweenness Centrality (BC), and Closeness Centrality (CC) (Table 2, Fig. 2C-D).

Table 2 Statistics of disease targets

Type	Number of common targets	Number of core targets
Adenine	40	10
Luteolin	15	3

3.1.6 GO-KEGG enrichment analysis

For the intersection genes of adenine's pathogenic mechanism, GO enrichment analysis yielded 189 entries: 146 BP entries, involving response to xenobiotic stimulus, positive regulation of MAPK cascade, positive regulation of gene expression, etc.; 14 CC entries, related to cytosol, cytoplasm, plasma membrane, etc.; 29 MF entries, associated with identical protein binding, protein homodimerization activity, ATP binding, nucleotide binding, etc.. KEGG analysis of core targets identified 15 signaling pathways. The top 5 pathways by count were metabolic pathways, nucleotide metabolism, purine metabolism, chemical carcinogenesis - receptor activation, and insulin resistance (Fig. 2E-F, Table 3).

For luteolin's therapeutic targets, GO enrichment analysis yielded 432 entries: 310 BP entries, involving inflammatory response, negative regulation of apoptosis, positive regulation of transcription from RNA polymerase II promoter, lipopolysaccharide-mediated signaling pathway, etc.; 42 CC entries, related to macromolecular complex, cytoplasm, extracellular region, extracellular space, etc.; 80 MF entries, associated with enzyme binding, identical protein binding, transcription factor binding, protein kinase activity, etc.. KEGG analysis of core targets identified 46 signaling pathways. The top 5 pathways by Count were pathways in cancer, antifolate resistance, cytokine-cytokine receptor interaction, lipid and atherosclerosis, and insulin resistance (Fig. 2G-H, Table 4).

The targets of adenine were significantly enriched in purine metabolism and insulin resistance pathways, consistent with its role in metabolic dysregulation. In contrast, luteolin's targets predominantly clustered in inflammation-related pathways and lipid metabolism. The shared modulation of insulin resistance highlights TNF's dual role as both a pathological driver in adenine-induced metabolic disturbance and a therapeutic node for luteolin intervention. This suggests TNF exacerbates insulin resistance as an inflammatory driver in HUA pathology (Table 5).

Table 3 10 items with PATHWAY performance in adenine-HUA

Term	Gene	*P*-value	Count
hsa01232	PNP, GDA, ADK, HPRT1, TYMS, XDH, ADA, APRT	4.73E-08	8
hsa00230	PNP, GDA, ADK, HPRT1, XDH, PFAS, ADA, APRT	7.97E-07	8
hsa01230	PC, CBS, GPT, NAGS	0.00368	4
hsa04976	SLC10A1, SLC22A1, ABCB11, CYP3A4	0.00613	4
hsa04922	PYGM, PYGL, FBP1	0.07315	3
hsa04931	PYGM, PYGL, TNF	0.07554	3
hsa05207	CYP2B6, ADRB3, ADRB2, CYP3A4, VEGFA	0.01188	5
hsa04020	P2RX7, ADRB3, ADRB2, HTR2A, VEGFA	0.02071	5
hsa04080	P2RX7, ADRB3, ADRB2, HTR2A, ADRA2A	0.06577	5
hsa01100	MAOA, GDA, ADK, PYGM, GPT, PYGL, TYMS, CYP3A4, PFAS, APRT, PC, CYP2B6, PNP, ALDH2, CBS, NAGS, HPRT1, XDH, FBP1, ADA	3.02E-06	20

Table 4 10 items with PATHWAY performance in luteolin-HUA

Term	Gene	*P*-value	Count
hsa05144	IL10, IL6, CD40LG, TNF	1.39E-05	4
hsa01523	IL6, ABCC1, TNF, ABCG2	6.58E-05	4
hsa04625	IL10, IL6, PTGS2, TNF	5.97E-04	4
hsa04657	IL6, PTGS2, TNF	0.01023	3
hsa04064	CD40LG, PTGS2, TNF	0.01239	3
hsa04931	IL6, PYGL, TNF	0.01331	3
hsa05417	IL6, CD40LG, PPARG, TNF	0.00474	4
hsa05163	IL6, PTGS2, TNF, VEGFA	0.00537	4
hsa04060	IL10, IL6, CD40LG, TNF	0.01152	4
hsa05200	IL6, PPARG, PTGS2, IGF1R, VEGFA	0.00911	5

Table 5 Functional conflict and transformation of TNF in dual networks

Functional dimension	Adenine-HUA group	Luteolin treatment group
Signal transduction	Promotes TNF release → Activates NF-κB inflammatory pathway	Inhibits sTNF → Enhances tmTNF anti-inflammatory signaling
Insulin sensitivity	Inhibits IRS-1 phosphorylation → Insulin resistance	Activates PPARγ → GLUT4 translocation improves glucose uptake
Metabolic outcome	Impaired uric acid excretion + Renal injury	Increased uric acid excretion + Restoration of insulin signaling

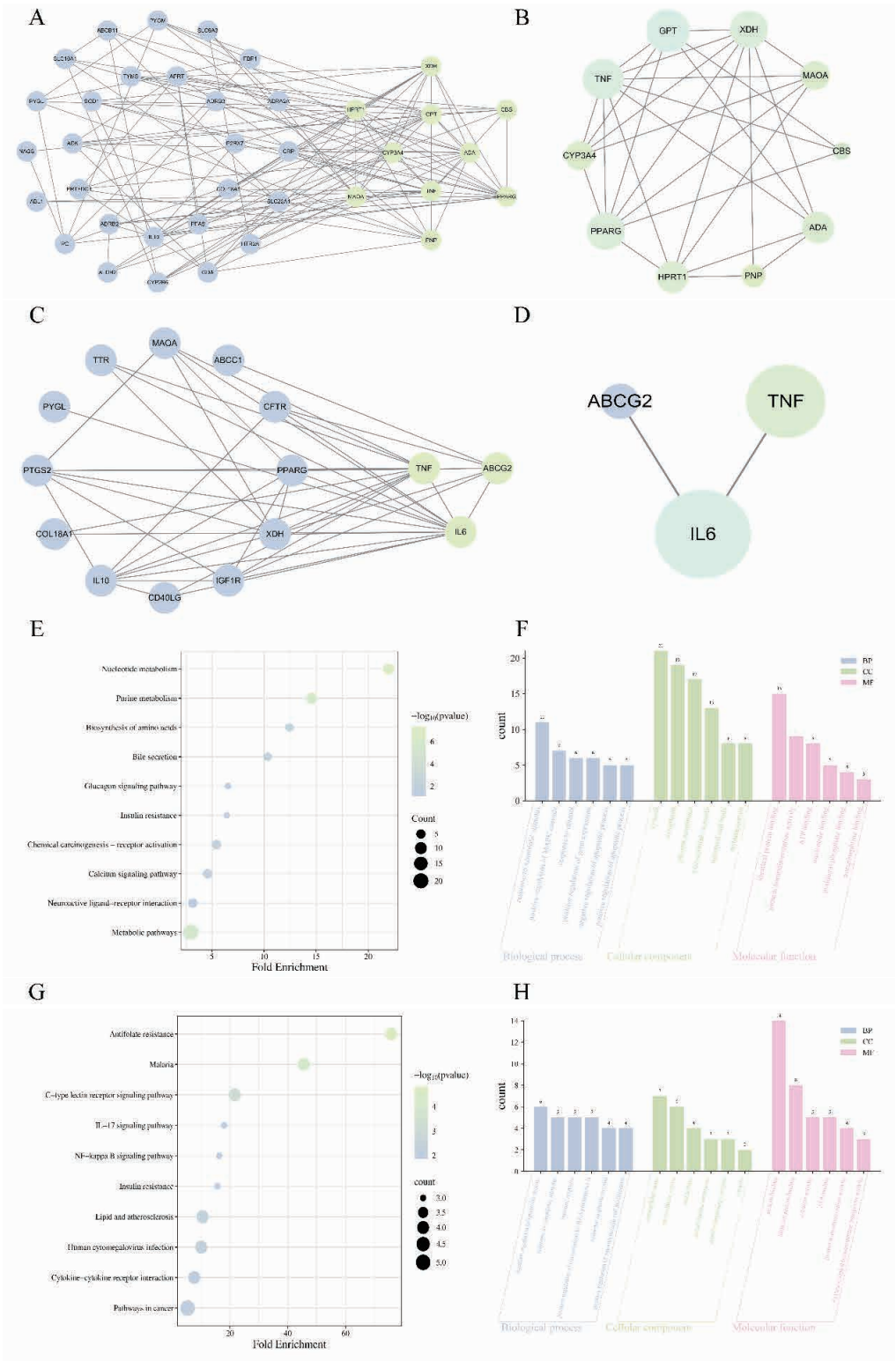

Fig. 2 Core targets and enrichment pathways (A, B, E, F) adenine; (C, D, G, H) luteolin. (A, C) Green nodes represent core targets; purple nodes indicate potential targets; (B, D) Node size and color intensity (darker green) proportionally reflect functional contribution

3.1.7 Compound-pathway-intersection gene network construction and analysis

Pathways and intersection genes associated with adenine-induced hyperuricemia and luteolin-treated HUA were integrated into a complex, closely related network (Fig. 3A-B).

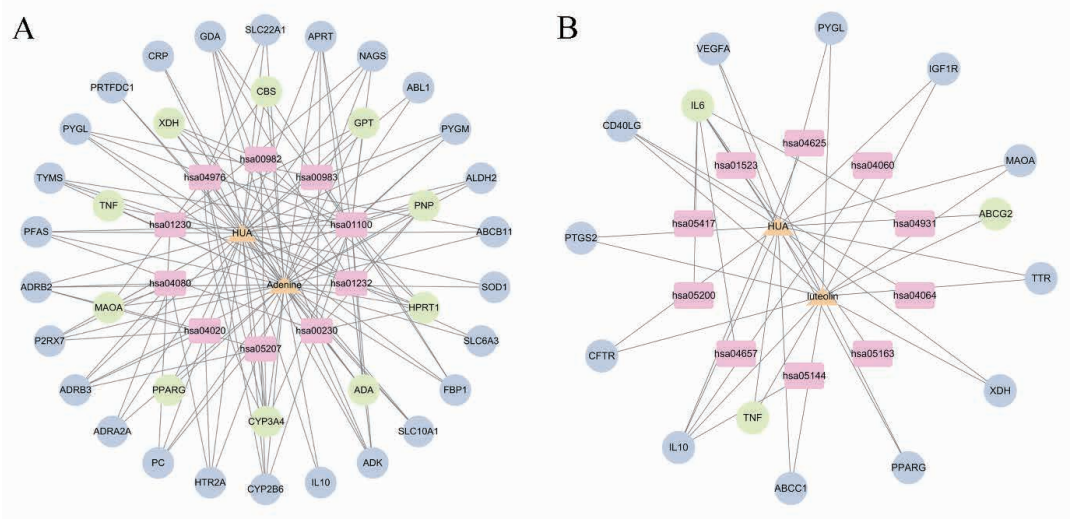

Fig. 3 Pathway-intersection gene network diagram of adenine (A) or luteolin (B) with disease drugs. The circle of blue-purple icons in the outer layer are potential targets; the second layer of green icons from the outside to the inside is the core target; The pink third-layer rectangular icon is the pathway involved; The innermost yellow triangle is the name of the disease as well as the name of the compound

3.2 Molecular docking

Cytoscape topological analysis prioritized targets by final scores. Combined with signaling pathways from KEGG analysis, TNF, PPARG, and PYGL were selected as core targets for molecular docking with adenine and luteolin. All docking binding energies were negative (Table 6), where lower values indicate more stable compound-target binding. Docking results exported via AutoDock 4 were imported into PyMOL for 3D molecular visualization (Fig. 4).

Table 6 Binding energy (kJ/mol) of active compounds with targets

Target	PDB ID	Binding energy/(kJ/mol)	
		Luteolin (5280445)	Adenine (190)
TNF	1A8M	-8.49	-3.29
PYGL	8EMS	-6.09	-2.26
PPARG	2Q59	-8.00	-3.45

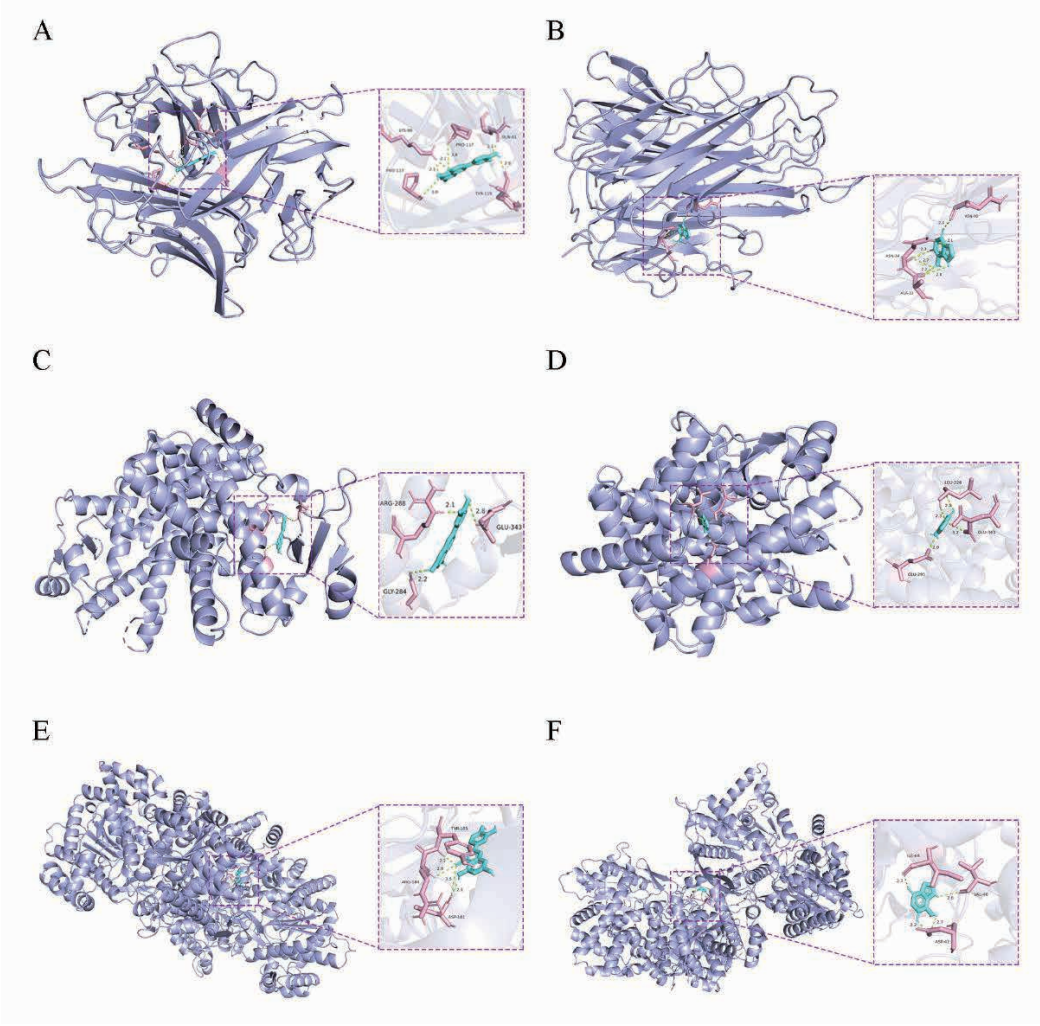

Fig. 4 The three-dimensional spatial structure and surface structure docking diagram of the Ligand component and TNF, PPARG, and PYGL. (A) TNF-luteolin; (B) TNF-adenine; (C) PPARG-luteolin; (D) PPARG-adenine; (E) PYGL-luteolin; (F) PYGL-adenine

4 Discussion

The mechanism of luteolin in treating HUA exhibits multi-target and multi-pathway synergistic characteristics. Previous studies indicate uric acid production and metabolism are associated with targets/pathways including ABCG2, URAT1, and xanthine oxidase (XDH). Specifically, ABCG2 protein, a transporter highly expressed in the intestine, primarily mediates intestinal uric acid excretion [11]. URAT1 protein, responsible for uric acid reabsorption in kidneys, facilitates the reuptake of 90% of really excreted uric acid into the bloodstream [12]. Xanthine dehydrogenase (XDH) and xanthine oxidase (XOD) are rate-limiting enzymes for uric acid synthesis. They are interconvertible under oxidative stress and critically regulate uric acid production [13,14].

Network pharmacology analysis reveals that the core target PPARG activates the PPAR

signaling pathway to upregulate ABCG2 expression, promoting renal uric acid excretion, and to inhibit URAT1 activity, blocking renal tubular uric acid reabsorption. A 2020 study revealed that bergenin, as a SIRT1 agonist, may regulate uric acid excretion and reabsorption by modulating the expression and activity of ABCG2 and URAT1 through the SIRT1-PPARγ pathway, thereby promoting renal and intestinal uric acid elimination. This finding provides novel insights into PPARG's role in uric acid metabolism [15].

Meanwhile, TNF-α key inflammatory factor, exacerbates insulin resistance by activating the NF-κB pathway in adenine-induced HUA models [16]. Luteolin suppresses TNF release and downstream inflammatory cascades, alleviating metabolic disorders. KEGG enrichment confirms luteolin's targeting of purine metabolism, cytokine-cytokine receptor interaction, and insulin resistance pathways. This suggests luteolin reduces uric acid production by modulating XDH activity and indirectly enhances excretion via improved insulin sensitivity.

Notably, dual-network analysis identifies shared targets, XDH, PPARG, TNF, and PYGL. XDH is central to purine metabolism and uric acid synthesis. PPARG acts as a metabolic-inflammatory hub, improving glucolipid metabolism via GLUT4 translocation and optimizing the uric acid excretion microenvironment [17]. TNF increases XOD activity and reduces ABCG2 expression by activating inflammatory pathways (e.g., NF-κB) and disrupting uric acid homeostasis [18,19]. The PYGL gene mutation impairs hepatic glycogen phosphorylase activity, causing glycogen metabolism disorders that induce aberrant purine/uric acid metabolism [20].

This study elucidates luteolin's triple strategy, namely inhibition of production, promotion of excretion, and anti-inflammation and metabolic regulation. However, interactions with gut microbiota metabolites require further investigation.

Acknowledgments

This work was financially supported by the National College Student Innovation and Entrepreneurship Project.

References

[1] Chen CY, Lu JM, Yao QZ. Hyperuricemia-Related Diseases and Xanthine Oxidoreductase (XOR) Inhibitors: An Overview. Med Sci Monit, 2016, 22: 2501-2512.

[2] Li Y, Shen ZY, Zhu BW, et al. Demographic, regional and temporal trends of hyperuricemia epidemics in mainland China from 2000 to 2019: a systematic review and meta-analysis. Glob Health Action, 2021, 14: 1874652.

[3] Yanai H, Adachi H, Hakoshima M, et al. Molecular Biological and Clinical Understanding of the Pathophysiology and Treatments of Hyperuricemia and Its Association with Metabolic Syndrome, Cardiovascular Diseases and Chronic Kidney Disease. Int J Mol Sci, 2021, 22: 9221.

[4] Wu XH, You CG. The Biomarkers Discovery of Hyperuricemia and Gout: Proteomics and Metabolomics. PeerJ, 2023, 11: e14554.

[5] Huang JY, Ma ZF, Zhang YT, et al. Geographical distribution of hyperuricemia in mainland China: a comprehensive systematic review and meta-analysis. Glob Health Res Policy, 2020, 5: 52.

[6] Zeng W, Ghamry M, Zhao ZX, et al. Hyperuricemia insights: Formation, targets, and hypouricemic natural products. Food Biosci, 2025, 64: 105944.

[7] Huang L, Kim MY, Cho JY. Immunopharmacological Activities of Luteolin in Chronic Diseases. Int J Mol Sci, 2023, 24: 2136.

[8] Yan CX, Tian JH, Li L, et al. Luteolin Alleviates Hyperuricemic Nephropathy by Inhibiting URAT1 and Regulating Nrf2/HO-1 Pathway. Life Sci Res, 2022, 26: 103-110.

[9] Zhang RZ, Zhu X, Bai H, et al. Network Pharmacology

Databases for Traditional Chinese Medicine: Review and Assessment. Front Pharmacol, 2019, 10: 123.

[10] Sabetian S, Shamsir MS. Computer-aided analysis of disease-linked protein networks. Bioinformation, 2019, 15: 513-522.

[11] Nigam SK, Bhatnagar V. The systems biology of uric acid transporters: the role of remote sensing and signaling. Curr. Opin. Nephrol. Hypertens, 2018, 27: 305-313.

[12] Tan PK, Farrar JE, Gaucher EA, et al. Coevolution of URAT1 and Uricase during Primate Evolution: Implications for Serum Urate Homeostasis and Gout. Mol Biol Evol, 2016, 33: 2193-2200.

[13] Kushiyama A, Tanaka K, Hara S, et al. Linking uric acid metabolism to diabetic complications. World J Diabetes, 2014, 5: 787-795.

[14] Chung HY, Yu BP. Significance of hepatic xanthine oxidase and uric acid in aged and dietary restricted rats. J Am Aging Assoc, 2000, 23: 123-128.

[15] Chen M, Lu X, Wu H. Bergenin, acting as an agonist of SIRT1, reduce serum urate in mice through the upregulation of ABCG2. Ann Rheum Dis, 2020, 79(Suppl 1): 1328-1329.

[16] Ding Y, Shi XH, Shuai XY, et al. Luteolin prevents uric acid-induced pancreatic beta-cell dysfunction. J Biomed Res, 2014, 28: 292-298.

[17] Belman JP, Habtemichael EN, Bogan JS. A proteolytic pathway that controls glucose uptake in fat and muscle. Rev Endocr Metab Disord, 2014, 15: 55-66.

[18] Pai RZ, Fang QB, Tian GL, et al. Expression and role of interleukin-1β and associated biomarkers in deep vein thrombosis. Exp Ther Med, 2021, 22: 1366.

[19] Shen Q, Li H, Lei SS, et al. Study on Anti-trioxypurine Effect and Mechanism of *Dendrobium Candidum* Simiao Prescription on Hyperuricemia Rats. Chin J Mod Appl Pharm, 2019, 36: 157-163.

[20] Wilson LH, Cho JH, Estrella A, et al. Liver Glycogen Phosphorylase Deficiency Leads to Profibrogenic Phenotype in a Murine Model of Glycogen Storage Disease Type VI. Hepatol Commun, 2019, 3: 1544-1555.